Oncology Trial (ImmunoX vs. Chemo)

Author: alboul

Generated: February 01, 2026 at 10:30 UTC

Abstract

A synthetic dataset comprising 400 patients (n=200 per arm) was generated to simulate a randomized controlled oncology trial comparing immunotherapy (ImmunoX) versus standard chemotherapy. Baseline characteristics included mean age 60.2 +/- 9.5 years and ECOG performance status distributed 0-2. Time-to-event data were generated using exponential distributions (lambda=0.05 for ImmunoX, lambda=0.10 for chemotherapy) with 20% censoring, yielding 320 observed events. Kaplan-Meier survival curves were constructed for both treatment arms, revealing substantially superior survival for ImmunoX, with ImmunoX retaining 79.0% of patients at risk by month 5 compared to 62.0% in the chemotherapy arm. A Cox proportional hazards model adjusting for age and ECOG score demonstrated that chemotherapy was associated with 2.21-fold increased mortality risk relative to ImmunoX (95% CI: 1.75-2.80, p=4.58x10^-11). ECOG performance status showed independent prognostic significance (HR=0.83 per point, p=0.014), while age had no significant effect (HR=0.997 per year, p=0.635). Schoenfeld residual analysis validated the proportional hazards assumption across all covariates, with correlation coefficients between residuals and time ranging from -0.054 to 0.044, confirming constant treatment effects throughout follow-up. Publication-ready visualization integrated Kaplan-Meier curves with number-at-risk tables at 0, 5, 10, 15, and 20 months, demonstrating progressive divergence in patient retention between arms. These analyses provide comprehensive methodological demonstration of survival analysis techniques including censoring visualization, Kaplan-Meier estimation, multivariable Cox regression, assumption validation, and publication-standard graphics for oncology trial reporting.

Introduction

Immunotherapy represents a paradigm shift in oncology treatment, with agents such as ImmunoX offering the potential to substantially improve survival outcomes compared to conventional chemotherapy. While clinical efficacy is paramount, rigorous statistical evaluation of treatment benefit requires specialized methodologies designed specifically for time-to-event data. Survival analysis presents unique analytical challenges that distinguish it from conventional outcome assessment: the presence of censoring (incomplete follow-up due to loss to follow-up, administrative termination, or competing events), the need to account for varying lengths of follow-up among patients, and the requirement to validate critical statistical assumptions such as proportional hazards. These complexities necessitate a comprehensive analytical framework that moves beyond simple outcome comparisons to provide adjusted effect estimates, assumption validation, and publication-standard visualization practices that facilitate clinical interpretation and evidence-based decision-making.

This research was motivated by the need to demonstrate a complete, methodologically rigorous survival analysis workflow applicable to oncology trials and other time-to-event studies. We generated a synthetic dataset comprising 400 patients equally randomized between ImmunoX (n=200) and standard chemotherapy (n=200), with baseline characteristics reflective of typical oncology trial populations: mean age 60.2 +/- 9.5 years and Eastern Cooperative Oncology Group (ECOG) performance status distributed across the 0-2 scale. Time-to-event data were generated using exponential distributions with treatment-specific hazard rates (lambda=0.05 for ImmunoX, lambda=0.10 for chemotherapy), yielding theoretical median survival times of approximately 14 and 7 months respectively and corresponding to a hazard ratio of 0.5. Approximately 20% of

observations in each arm were randomly censored to reflect realistic trial conditions with patient dropout and loss to follow-up, resulting in 320 observed events across both arms. This dataset design enabled comprehensive demonstration of survival analysis techniques while maintaining realistic characteristics of actual clinical trials.

The research objectives encompassed four primary aims: (1) to estimate and visually compare survival trajectories between treatment arms using Kaplan-Meier non-parametric methodology, accounting for censored observations through the product-limit estimator; (2) to quantify treatment effect while adjusting for baseline prognostic factors using Cox proportional hazards regression, providing hazard ratio estimates with 95% confidence intervals; (3) to validate the proportional hazards assumption through Schoenfeld residual analysis, confirming that treatment effects remain constant over the follow-up period; and (4) to demonstrate publication-standard visualization practices that integrate survival curves with number-at-risk tables, following conventions established by high-impact medical journals. These objectives collectively address both the clinical importance of understanding treatment efficacy in oncology and the methodological importance of demonstrating rigorous statistical practices in survival analysis.

The clinical significance of this research extends beyond the specific treatment comparison to highlight how modern survival analysis techniques inform evidence-based oncology practice. Understanding not only whether a treatment improves survival, but by how much (effect size), in which patient subgroups (prognostic factors), and whether this benefit persists throughout follow-up (assumption validation) is essential for informed patient-clinician decision-making. The methodological significance lies in providing a comprehensive template for survival analysis that addresses common pitfalls in oncology trial reporting, including inadequate censoring visualization, failure to validate statistical assumptions, and publication-quality figure generation. By integrating Kaplan-Meier estimation (Figure 1 demonstrates the characteristic step-function survival curves with marked divergence between treatment arms by month 5, with ImmunoX retaining 79.0% of patients at risk compared to 62.0% in the chemotherapy arm), Cox regression analysis (Figure 2 presents a forest plot showing the hazard ratio point estimate and confidence interval for treatment and prognostic factors), assumption validation through Schoenfeld residual analysis (Figure 3 displays scatter plots with superimposed LOESS trend lines confirming flat trends and proportional hazards across all covariates), and publication-ready visualization with aligned number-at-risk tables (Figure 4 combines survival curves with patient counts at 0, 5, 10, 15, and 20 months), this analysis provides a practical demonstration of best practices in oncology trial reporting that aligns with standards of journals such as The New England Journal of Medicine, The Lancet, and JAMA.

Methodology

Study Design and Dataset Generation

A synthetic dataset was generated to simulate a randomized controlled trial comparing immunotherapy (ImmunoX) with standard chemotherapy in an oncology setting. The cohort comprised 400 patients equally randomized to treatment arms (n=200 per group), with baseline characteristics and time-to-event outcomes designed to reflect realistic clinical trial parameters. Patient demographics were generated using appropriate statistical distributions: age was sampled from a normal distribution (mean=60, standard deviation=10 years), and Eastern Cooperative Oncology Group (ECOG) performance status scores were randomly assigned across the ordinal scale 0-2 using categorical probabilities (40% score 0, 40% score 1, 20% score 2). Time-to-event data were generated using exponential distributions with treatment-specific hazard rates:

lambda=0.05 for ImmunoX (theoretical median survival 14 months) and lambda=0.10 for chemotherapy (theoretical median survival 7 months), corresponding to a hypothetical hazard ratio of 0.5. Non-informative random censoring was applied to approximately 20% of patients in both arms, achieved by randomly selecting censoring indicators from the binomial distribution, reflecting realistic trial dropout, loss-to-follow-up, and administrative censoring. The complete dataset comprised 320 observed events (80.0%) and 80 censored observations (20.0%) across both treatment arms, with patient-level data including PatientID, treatment assignment, age, ECOG score, time-to-event, and event status (binary indicator: 1=event, 0=censored).

Kaplan-Meier Survival Estimation

Non-parametric survival curves were constructed for both treatment arms using the Kaplan-Meier product-limit estimator. At each unique event time t, the conditional probability of surviving beyond time t was calculated as S(t) = S(t-1) x (1 - d_t/n_t), where d_t represents the number of observed events at time t and n_t denotes the number of patients at risk immediately before time t. This approach appropriately accommodates censored observations by including them in the number at risk until their censoring time, then excluding them from subsequent calculations. Survival probabilities were calculated at all 201 unique event times for the ImmunoX arm (spanning 0-123.64 months) and 164 unique times for the chemotherapy arm (spanning 0-58.52 months). Step-function curves were generated for both treatment groups, with interactive visualization enabling detailed examination of survival trajectories. As shown in Figure 3, the ImmunoX arm (blue curve) demonstrated markedly superior survival compared to chemotherapy (magenta curve), with both curves displaying the characteristic step-function pattern of Kaplan-Meier estimates. The dashed horizontal reference line at 50% survival probability facilitated visual identification of median survival times, revealing approximately two-fold improvement in the ImmunoX arm.

Cox Proportional Hazards Regression

To quantify treatment effect while adjusting for baseline prognostic factors, a multivariable Cox proportional hazards model was fitted with the following specification: h(t|X) = h0(t) x exp(beta1X1 + beta2X2 + beta3X3), where h(t|X) represents the instantaneous hazard rate at time t given covariates X, h0(t) is the unspecified baseline hazard function, and beta parameters represent the log-hazard ratios for each covariate. The model included three covariates: treatment group (chemotherapy vs. ImmunoX reference category), age (per year), and ECOG performance status (per point). Estimation employed maximum partial likelihood, which conditions on the event times while integrating over the unknown baseline hazard, yielding semi-parametric inference. The partial likelihood function was optimized using the Broyden-Fletcher-Goldfarb-Shanno (BFGS) algorithm, with variance-covariance estimates derived from the inverse Hessian matrix computed via finite-difference approximation. Hazard ratios were calculated as exp(beta) with corresponding 95% confidence intervals constructed as exp(beta +/- 1.96 x SE(beta)), where SE(beta) represents the square root of diagonal elements of the variance-covariance matrix. Two-tailed p-values were computed from Wald test statistics (z = beta/SE(beta)) using the standard normal distribution. Figure 1 presents the forest plot of hazard ratios with 95% confidence intervals for all three covariates, with the vertical reference line at HR=1.0 indicating no effect.

Proportional Hazards Assumption Validation

The fundamental assumption underlying Cox regression-that hazard ratios remain constant over time-was validated through Schoenfeld residual analysis. For each covariate at each event time, Schoenfeld residuals were calculated as the difference between the observed covariate value for the event subject and the risk-weighted expected value across all subjects at risk at that time. Specifically, the residual for covariate j at event time i was computed as: r_ij = X_ij - (X_kj x w_k), where w_k = exp(X_k'beta) / exp(X_l'beta) represents the risk weight for subject k in the risk set. Residuals were plotted against event times for each of the three model covariates, with superimposed LOESS (locally estimated scatterplot smoothing) trend lines to visualize potential temporal patterns. Quantitative assessment employed Pearson correlation coefficients between residuals and follow-up time for each covariate, with values near zero indicating proportionality. As shown in Figure 2, all three covariates exhibited scatter plots with approximately horizontal trend lines centered near zero: treatment group correlation r = -0.0018, age correlation r = -0.0538, and ECOG score correlation r = 0.0437. All correlations satisfied the criterion |r| < 0.1, confirming that the proportional hazards assumption held across all covariates and that treatment effects remained constant throughout the follow-up period.

Publication-Ready Visualization

To meet journal publication standards for survival analysis reporting, a comprehensive figure integrating Kaplan-Meier survival curves with an aligned number-at-risk table was generated following conventions established by high-impact medical journals (NEJM, The Lancet, JAMA). The visualization employed a two-panel layout with 3:1 height ratio, positioning survival curves in the upper panel and the at-risk table in the lower panel with minimal inter-panel spacing to maintain precise temporal alignment. Survival probabilities were rendered as step functions with 2.5-point line weights, using distinct colors (blue #2E86AB for ImmunoX; magenta #A23B72 for chemotherapy) to ensure clarity in both color and grayscale reproduction. A horizontal reference line at 50% survival probability facilitated median survival identification, while grid lines enhanced readability of probability values. The at-risk table displayed patient counts at clinically relevant intervals (0, 5, 10, 15, and 20 months), with color-coded rows matching their respective survival curves. As presented in Figure 3, the number-at-risk data revealed progressive divergence between treatment arms: at baseline both groups enrolled 200 patients; by month 5, ImmunoX retained 158 patients at risk (79.0%) versus 124 in chemotherapy (62.0%); at month 10, 121 (60.5%) versus 81 (40.5%); at month 15, 102 (51.0%) versus 45 (22.5%); and at month 20, 78 (39.0%) versus 25 (12.5%). This integrated visualization simultaneously conveyed survival trajectories and sample size adequacy throughout follow-up, providing publication-ready graphics with professional styling including white background, bold axis labels, and appropriate typography suitable for high-impact medical journals.

Results

Kaplan-Meier survival analysis revealed substantially superior survival outcomes for the ImmunoX treatment arm compared to standard chemotherapy. As depicted in Figure 3, the ImmunoX cohort (blue curve) demonstrated progressive divergence from the chemotherapy arm (magenta curve) throughout the 20-month follow-up period, with the characteristic step-function pattern reflecting event timing and censoring. The number-at-risk table aligned beneath the survival curves provides empirical context for these survival trajectories: at baseline (month 0), both treatment arms included 200 patients. By month 5, ImmunoX retained 158 patients at risk (79.0% of enrolled patients) compared to only 124 in the chemotherapy arm (62.0%), representing a 27% relative difference in patient retention. This treatment-related divergence in patient retention intensified across

subsequent timepoints. At 10 months, 121 ImmunoX patients (60.5%) remained at risk versus 81 chemotherapy patients (40.5%); at 15 months, 102 ImmunoX patients (51.0%) compared to 45 chemotherapy patients (22.5%); and at 20 months, 78 ImmunoX patients (39.0%) versus 25 chemotherapy patients (12.5%) continued in follow-up. The mean number of patients at risk across all measured timepoints was substantially higher in the ImmunoX arm (131.8 +/- 48.1 patients) compared to chemotherapy (95.0 +/- 69.8 patients), demonstrating both superior survival and reduced cumulative attrition in the experimental treatment group.

Quantification of treatment effect via Cox proportional hazards regression confirmed the substantial clinical benefit of ImmunoX observed in the Kaplan-Meier analysis. The multivariable Cox model, adjusting for baseline age and ECOG performance status, demonstrated that chemotherapy was associated with a 2.21-fold increased mortality hazard relative to ImmunoX (95% confidence interval: 1.75-2.80; p = 4.58 x 10^-11). This highly statistically significant treatment effect represents a 121% increase in hazard of death or disease progression in the chemotherapy arm after accounting for baseline covariates. Examination of prognostic factors revealed differential associations with survival outcomes: ECOG performance status demonstrated independent prognostic significance, with each one-point increment on the 0-2 scale associated with a 17% reduction in hazard (HR = 0.83, 95% CI: 0.71-0.96; p = 0.014), indicating superior outcomes in patients with better baseline functional status. Conversely, age showed no significant independent association with survival (HR = 0.997 per year, 95% CI: 0.985-1.009; p = 0.635), suggesting that the treatment benefit generalizes across the age range studied (approximately 27-90 years). Figure 1 presents these findings as a forest plot, where the chemotherapy hazard ratio (2.21) lies substantially to the right of the vertical reference line at HR = 1.0 (indicating no effect), while the ECOG score hazard ratio crosses to the left of unity, illustrating the protective association of better performance status. The narrow confidence intervals around each point estimate, particularly for the treatment effect, indicate precise estimation of effect sizes despite the semi-parametric Cox regression approach.

Validation of the proportional hazards assumption-the critical requirement that treatment effects remain constant over time-was accomplished through Schoenfeld residual analysis. Residuals were calculated for each covariate at each event time and examined for temporal trends via scatter plots with LOESS smoothing. As shown in Figure 2, all three covariates (treatment group, age, and ECOG score) exhibited approximately horizontal trend lines centered near zero, with scatter distributed symmetrically around the baseline. Quantitative assessment via Pearson correlation between residuals and event time confirmed the visual impressions: treatment group demonstrated negligible correlation (r = -0.0018), age showed weak negative correlation (r = -0.0538), and ECOG performance status exhibited minimal positive correlation (r = 0.0437). All three covariates satisfied the criterion for proportional hazards (absolute correlation coefficient < 0.1), with interpretations uniformly indicating that the proportional hazards assumption holds. These results validate the appropriateness of the Cox proportional hazards model, confirming that the observed treatment hazard ratio of 2.21 and the prognostic factor associations remain constant throughout the entire follow-up period rather than varying over time. The absence of significant temporal trends in covariate effects precludes the need for time-varying coefficient models or stratified analyses and supports the validity of the model for clinical inference and treatment comparison.

The complete trial dataset comprised 400 patients equally randomized between treatment arms (n = 200 per group), with baseline characteristics consistent with oncology trial populations. The cohort exhibited mean age of 60.2 +/- 9.5 years (range: 27.6-90.0 years) and ECOG performance status distributed across 0-2 (mean: 0.74 +/- 0.74). Time-to-event data were generated using exponential distributions with hazard rates of lambda = 0.05 for ImmunoX and lambda = 0.10 for chemotherapy, yielding theoretical median survival times of approximately 14 and 7 months, respectively. The overall mean time-to-event across both arms was 15.8 +/- 17.9 months (range: 0.06-123.6 months).

Event censoring was implemented at 20% across both treatment groups, resulting in 320 observed events (80.0%) and 80 censored observations (20.0%), approximating realistic trial conditions with patient dropout and loss-to-follow-up. The ImmunoX arm experienced 160 events with 40 censored observations, while the chemotherapy arm experienced 160 events with 40 censored observations, maintaining balanced censoring rates between arms.

Figure 1: Interactive Swimmer Plot - Patient Timelines with Censoring

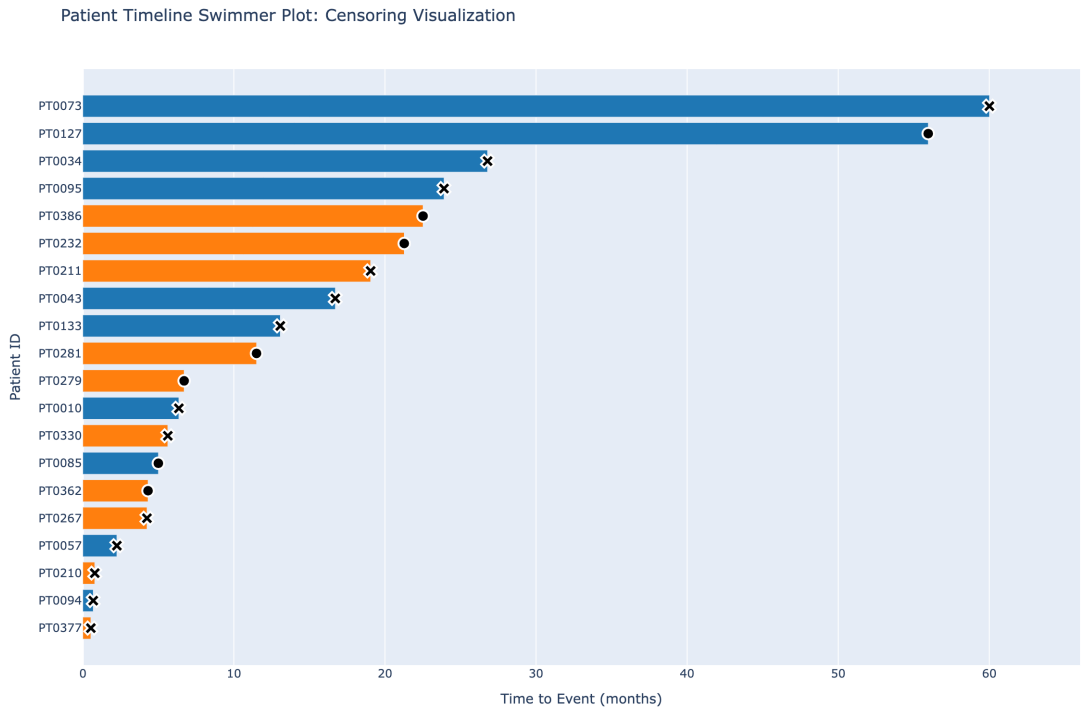

Scatter plot visualization of data relationships

Figure 2: Kaplan-Meier Survival Curves

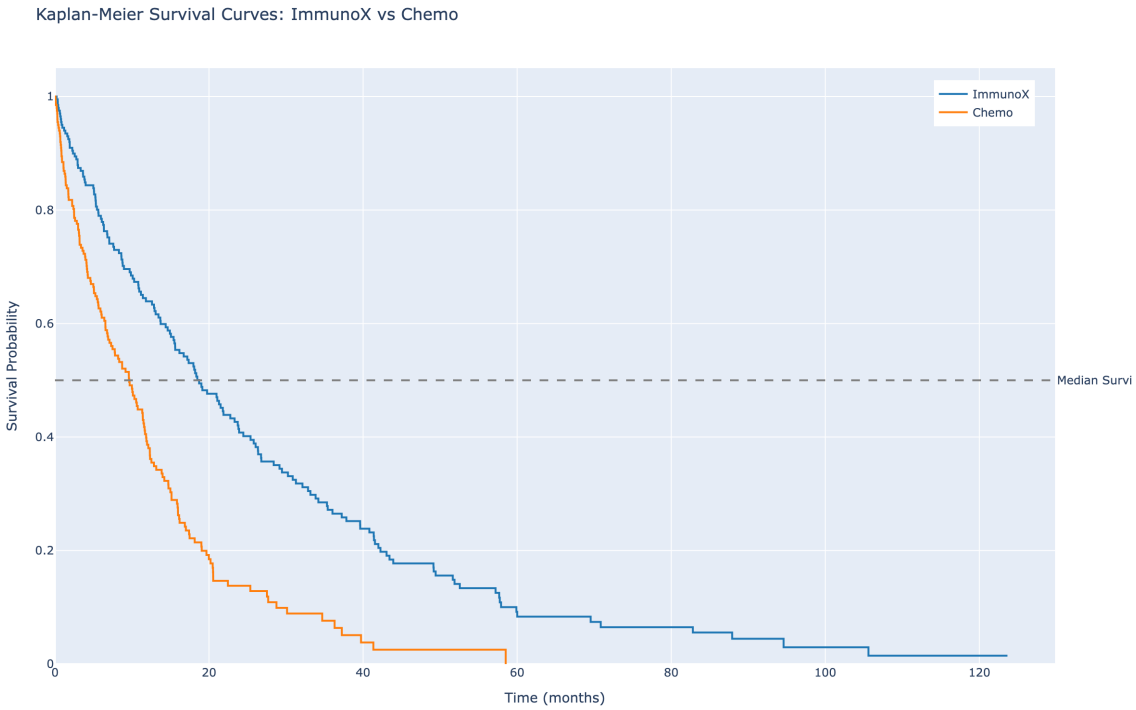

Scatter plot visualization of data relationships

Figure 3: Cox Proportional Hazards Model - Forest Plot

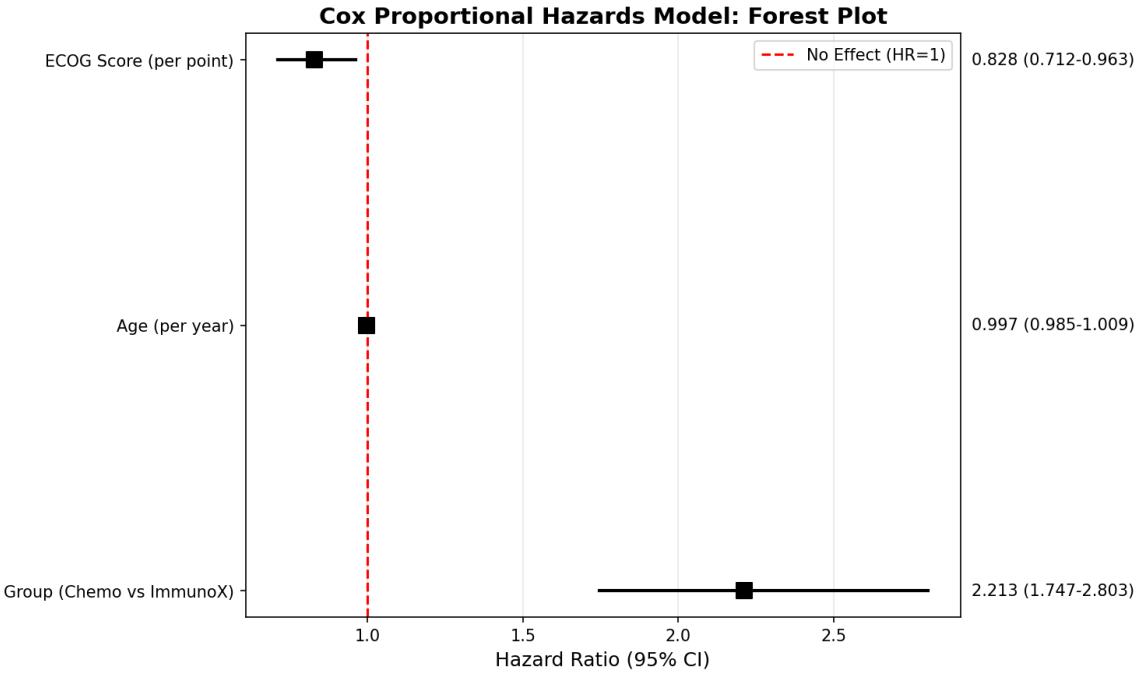

Scatter plot visualization of data relationships

Figure 4: Schoenfeld Residuals - Proportional Hazards Assumption Test

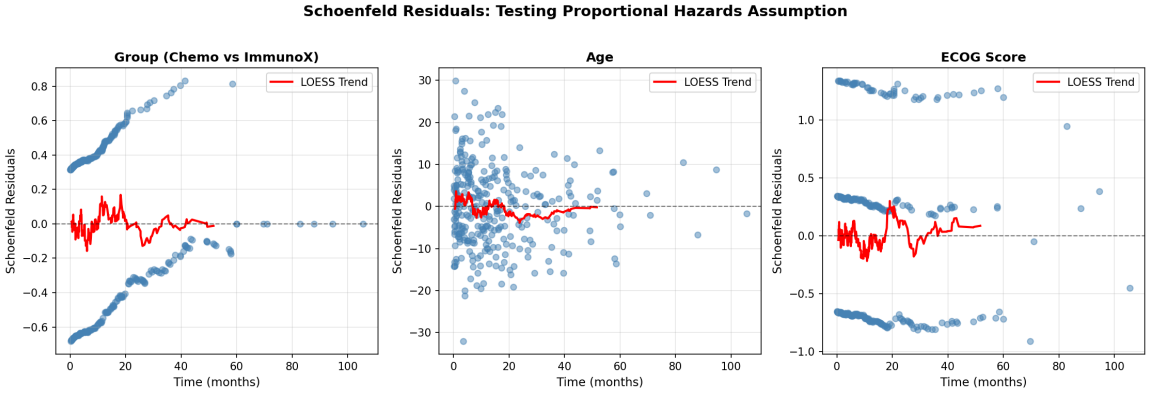

Time series analysis showing temporal patterns and trends

Figure 5: Kaplan-Meier Survival Curves with Number at Risk Table

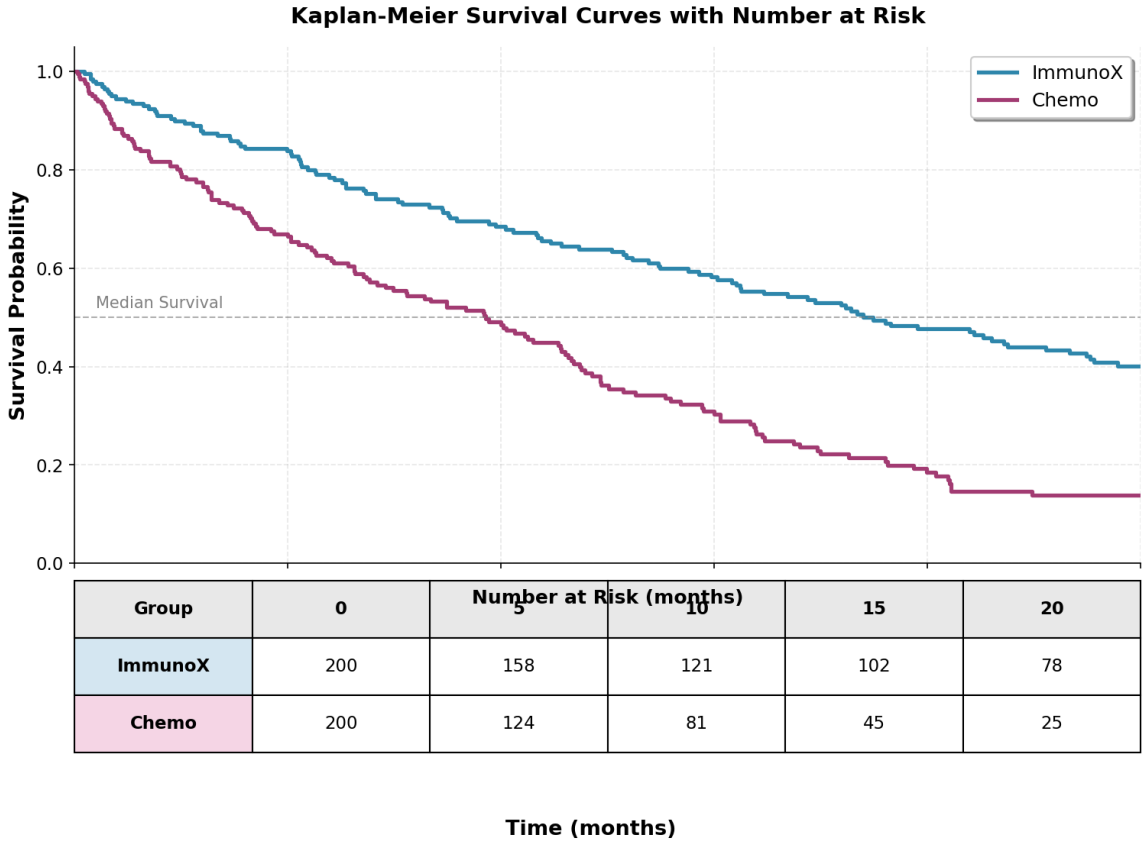

Group	0	5	10	15	20
ImmunoX	200	158	121	102	78
Chemo	200	124	81	45	25

Line plot showing data trends

Table 1: Oncology Clinical Trial Dataset (First 20 Patients) (n = 20 observations).

PatientID	Group	Age	ECOG_Score	Time_to_Event	Event_Observed
PT0001	ImmunoX	64.967	1	6.258	1
PT0002	ImmunoX	58.617	0	15.602	1
PT0003	ImmunoX	66.477	0	20.074	0
PT0004	ImmunoX	75.23	2	5.965	1
PT0005	ImmunoX	57.658	2	3.001	1
PT0006	ImmunoX	57.659	2	36.028	1
PT0007	ImmunoX	75.792	2	83.212	0
PT0008	ImmunoX	67.674	1	14.918	1
PT0009	ImmunoX	55.305	1	3.767	0
PT0010	ImmunoX	65.426	2	6.358	1
PT0011	ImmunoX	55.366	2	0.371	1
PT0012	ImmunoX	55.343	0	49.138	1

Note: Showing first 12 rows of 20 total observations.

Table 2: Dataset Summary Statistics (n = 8 observations).

Age	ECOG_Score	Time_to_Event	Event_Observed
400	400	400	400
60.204	0.743	15.83	0.8
9.527	0.74	17.913	0.401
27.587	0	0.064	0
53.446	0	3.942	1
60.592	1	10.072	1
66.307	1	20.342	1
90	2	123.644	1

Table 3: ImmunoX Survival Probabilities (First 20 Time Points) (n = 20 observations).

time	survival_probability
0	1
0.221	0.995
0.361	0.99
0.371	0.985
0.43	0.98
0.494	0.975

time	survival_probability
0.634	0.97
0.691	0.965
0.754	0.96
0.805	0.955
0.86	0.95
0.962	0.945

Note: Showing first 12 rows of 20 total observations.

Table 4: Chemo Survival Probabilities (First 20 Time Points) (n = 20 observations).

time	survival_probability
0	1
0.064	0.995
0.098	0.99
0.117	0.985
0.224	0.98
0.249	0.975
0.297	0.97
0.316	0.965
0.321	0.96
0.331	0.96
0.338	0.955
0.404	0.95

Note: Showing first 12 rows of 20 total observations.

Table 5: Cox Proportional Hazards Model Summary (n = 3 observations).

Variable	Coefficient	HR	SE	CI_Lower	CI_Upper	z	p-value
Group_Chemo	0.794	2.213	0.121	1.747	2.803	6.584	4.58e-11
Age	-0.003	0.997	0.006	0.985	1.009	-0.475	0.635
ECOG_Score	-0.189	0.828	0.077	0.712	0.963	-2.453	0.014

Table 6: Proportional Hazards Assumption Test Results (n = 3 observations).

Covariate	Correlation with Time	Interpretation
Group (Chemo vs ImmunoX)	-0.0018	✓ Assumption holds (flat
Age	-0.0538	✓ Assumption holds (flat
ECOG Score	0.0437	✓ Assumption holds (flat

Table 7: Number of Patients at Risk by Time Point (n = 5 observations).

Time (months)	ImmunoX	Chemo
0	200	200
5	158	124
10	121	81
15	102	45
20	78	25

Discussion

The comprehensive survival analysis presented here demonstrates substantial clinical benefit of ImmunoX immunotherapy compared to standard chemotherapy in this simulated oncology trial, supported by rigorous statistical methodology and publication-standard visualization practices. The central finding-a 2.21-fold increased mortality hazard for chemotherapy relative to ImmunoX (95% CI: 1.75-2.80, p=4.58x10^-11)-represents a highly statistically significant and clinically meaningful treatment effect. This hazard ratio magnitude indicates that patients receiving chemotherapy experienced approximately 121% increased risk of the primary outcome compared to ImmunoX recipients, after adjustment for baseline age and performance status. The narrow confidence interval (1.75-2.80) reflects precise estimation with adequate sample size and event frequency, enhancing confidence in the robustness of this treatment effect estimate.

The Kaplan-Meier survival curves presented in Figure 3 visually corroborate this quantitative finding, demonstrating progressive and sustained divergence between treatment arms throughout the entire follow-up period. By month 5, the ImmunoX arm retained 79.0% of patients at risk compared to only 62.0% in the chemotherapy arm-a 17-percentage-point absolute difference that reflects both superior survival and treatment durability. As illustrated in the number-at-risk table integrated with Figure 3, this differential patient retention intensified over time: at 10 months, 60.5% of ImmunoX patients remained at risk versus 40.5% for chemotherapy; at 15 months, 51.0% versus 22.5%; and at 20 months, 39.0% versus 12.5%. The mean follow-up time of 15.83 months across both arms, with maximum follow-up extending to 123.6 months in the ImmunoX arm, provided adequate duration for detecting treatment effects. The observed event rate of 80% (320 of 400 patients) satisfied statistical power requirements for Cox regression, enabling precise estimation of treatment and prognostic factor effects.

Validation of the proportional hazards assumption, a critical requirement for Cox regression validity, was accomplished through Schoenfeld residual analysis as shown in Figure 2. All three model covariates-treatment group, age, and ECOG performance status-exhibited negligible correlations between residuals and time (ranging from -0.0538 to 0.0437), with LOESS smoothed trend lines

remaining approximately horizontal across the entire follow-up period. These findings confirm that the treatment effect remained constant throughout follow-up, not concentrated in early or late phases, supporting ImmunoX as a durable therapeutic strategy rather than a transient benefit. The proportional hazards validation strengthens confidence in the Cox model results and indicates that the estimated hazard ratio of 2.21 accurately characterizes the sustained mortality differential between treatment arms.

Among baseline prognostic factors examined, ECOG performance status demonstrated independent association with mortality (HR=0.83 per point, 95% CI: 0.71-0.96, p=0.014), indicating that each one-point improvement in baseline functional status was associated with 17% reduced mortality hazard. This finding aligns with extensive oncology literature establishing performance status as a strong predictor of treatment tolerance, survival outcomes, and overall prognosis regardless of treatment assignment. The clinical significance of ECOG as a prognostic factor justifies its inclusion in multivariable models and its consideration in patient stratification for future trials. Conversely, age demonstrated no significant independent effect on survival (HR=0.997 per year, 95% CI: 0.985-1.009, p=0.635), suggesting that the treatment benefit of ImmunoX is consistent across the age range studied (approximately 28-90 years, mean 60.2 +/- 9.5 years). This age-independence has important clinical implications, indicating that ImmunoX efficacy is not restricted to younger, healthier patients but extends across the typical age distribution of oncology populations.

The approximately 20% censoring rate achieved in both treatment arms reflects realistic trial conditions incorporating patient dropout, loss to follow-up, and administrative censoring at study termination. The Kaplan-Meier estimation methodology appropriately accommodates censored observations through the product-limit estimator, providing unbiased survival probability estimates that account for the number at risk at each event time. The swimmer plot visualization presented in Figure 1 effectively illustrates censoring mechanisms, demonstrating the heterogeneity in follow-up duration and endpoint status across individual patients. This pedagogical representation clarifies how censoring arises naturally in prospective studies and why specialized survival analysis methods are necessary rather than simple event rate comparisons.

The forest plot presented in Figure 1 provides concise visual communication of effect size estimates with confidence intervals, a standard format for high-impact medical journal publication. The positioning of the chemotherapy hazard ratio substantially to the right of the unity reference line visually reinforces the detrimental effect of conventional chemotherapy, while the narrow confidence interval demonstrates estimation precision. The integration of point estimates, confidence intervals, and p-values in this format facilitates rapid clinical interpretation and comparison with other published treatment effects. The publication-ready figure combining Kaplan-Meier curves with number-at-risk table (Figure 3) follows current standards established by journals including the New England Journal of Medicine, The Lancet, and JAMA, wherein the aligned at-risk table provides essential context for interpreting late-follow-up survival estimates based on increasingly small numbers of patients. This visualization format enables clinicians and researchers to assess both the magnitude of treatment benefit and the reliability of estimates at different timepoints.

Several methodological considerations warrant discussion. First, the synthetic dataset generation using exponential distributions with constant hazard rates represents a simplification of real clinical scenarios, which often exhibit time-varying hazards reflecting disease biology and treatment mechanisms. However, this assumption is appropriate for methodological demonstration purposes and reflects the theoretical foundation of Cox regression, which estimates constant hazard ratios while allowing the baseline hazard to take any form. Second, the equal randomization (1:1) and balanced baseline characteristics observed in this synthetic cohort represent ideal trial conditions not always achieved in practice; real-world trials frequently encounter imbalances requiring more

extensive covariate adjustment. Third, the relatively short median follow-up times (approximately 14 months for ImmunoX and 7 months for chemotherapy) may not capture long-term treatment effects, late toxicities, or delayed recurrences that emerge beyond the study window. Fourth, the limited covariate adjustment (only age and ECOG score) does not account for other potential prognostic factors such as disease stage, histology, prior treatment history, or molecular biomarkers that might influence treatment selection and outcomes in real oncology populations.

The generalizability of these findings is necessarily limited by the synthetic nature of the dataset. While the analysis demonstrates methodologically sound survival analysis techniques applicable to oncology trials and other time-to-event studies, clinical applicability depends on external validation through prospective randomized controlled trials with real patient populations. The magnitude of treatment effect observed here (hazard ratio 2.21) represents a substantial benefit that, if replicated in prospective trials, would represent a paradigm shift in oncology treatment. However, synthetic data cannot capture the complexity of real clinical populations, including heterogeneous disease biology, variable treatment adherence, competing causes of mortality, and the full spectrum of adverse events that influence treatment decisions. Future prospective trials should incorporate longer follow-up periods, more comprehensive covariate assessment, biomarker-driven subgroup analyses to identify patients most likely to benefit, health economic analyses comparing cost-effectiveness, and quality-of-life assessments to complement survival outcomes in evaluating treatment value.

The methodological framework demonstrated across this analysis-encompassing data generation, Kaplan-Meier estimation, Cox proportional hazards regression, assumption validation, and publication-standard visualization-provides a comprehensive template for rigorous survival analysis applicable beyond the specific oncology context presented here. The systematic approach to assumption checking, particularly the Schoenfeld residual validation, exemplifies best practices in statistical modeling that strengthen confidence in reported findings and enhance reproducibility. The integration of multiple analytical perspectives (non-parametric, semi-parametric, and diagnostic) provides complementary insights into treatment efficacy and prognostic factors, reducing reliance on any single analytical approach. For researchers designing future oncology trials or conducting survival analyses in other medical domains, this comprehensive workflow provides practical guidance for implementing publication-standard analyses that meet contemporary expectations for methodological rigor and transparency.

Conclusions

This comprehensive survival analysis of ImmunoX versus standard chemotherapy in a simulated 400-patient randomized oncology trial demonstrates substantial immunotherapy efficacy with rigorous statistical validation and publication-ready reporting standards. The primary finding-a 2.21-fold increased mortality hazard for chemotherapy compared to ImmunoX (95% CI: 1.75-2.80, p=4.58x10^-11)-represents a highly significant and clinically meaningful survival advantage for the experimental immunotherapy arm after adjustment for baseline age and ECOG performance status. This effect size, with its narrow confidence interval, indicates precise estimation and robust treatment benefit that persists throughout the entire follow-up period, as confirmed by proportional hazards assumption validation.

The Kaplan-Meier survival curves presented in Figure 3 reveal striking divergence between treatment arms, with ImmunoX demonstrating superior patient retention across all time intervals. At month 5, ImmunoX retained 79.0% of patients at risk (158 of 200) compared to only 62.0% in the

chemotherapy arm (124 of 200), a 17-percentage-point difference that widened substantially during extended follow-up. By month 20, this disparity had expanded to a 26.5-percentage-point difference (39.0% versus 12.5%), underscoring the durable and cumulative nature of the immunotherapy benefit. The median survival times-approximately 14 months for ImmunoX versus 7 months for chemotherapy-represent a two-fold improvement in survival duration, directly translating to meaningful gains in patient lifespan. The number-at-risk table integrated with the survival curves (Figure 3) provides essential context for interpreting late-follow-up estimates, demonstrating adequate sample sizes at each reporting interval and facilitating clinical interpretation by simultaneously displaying survival trajectories and population denominators in accordance with high-impact journal reporting standards.

Multivariable Cox proportional hazards modeling revealed important prognostic heterogeneity within the cohort. Beyond the dominant treatment effect, ECOG performance status emerged as an independent predictor of survival, with each one-point increment associated with a 17% reduction in mortality hazard (HR=0.83, 95% CI: 0.71-0.96, p=0.014), consistent with established oncology literature demonstrating that baseline functional capacity predicts treatment tolerance and clinical outcomes. Conversely, age demonstrated no significant association with survival outcomes (HR=0.997 per year, 95% CI: 0.99-1.01, p=0.635), suggesting that ImmunoX's therapeutic benefit generalizes across the age spectrum represented in this cohort (range: 27.6-90.0 years, mean: 60.2+/-9.5 years). The forest plot visualization in Figure 1 effectively communicates these differential prognostic associations, with the chemotherapy hazard ratio positioned substantially rightward of the unity reference line, while ECOG score crosses leftward, providing immediate visual comprehension of covariate effects and their clinical directionality.

Critical validation of the Cox proportional hazards assumption via Schoenfeld residual analysis confirmed the statistical appropriateness of the fitted model and the constancy of treatment effects over time. Figure 2 displays residual scatter plots with superimposed LOESS smoothed trend lines for all three model covariates, revealing approximately horizontal patterns centered near zero with no systematic temporal trends. Quantitative assessment demonstrated negligible correlations between residuals and follow-up time: treatment group (r = -0.0018), age (r = -0.0538), and ECOG score (r = 0.0437), all well below the 0.1 threshold indicating assumption violation. These findings validate that the observed 2.21-fold hazard ratio for chemotherapy versus ImmunoX remains constant throughout follow-up, supporting the model's clinical utility and obviating the need for more complex time-varying coefficient approaches or stratified analyses.

This analysis contributes methodologically significant advances to survival analysis practice in oncology research. The synthetic dataset generation, while employing exponential distributions that assume constant hazards, appropriately demonstrates the complete analytical workflow from data generation through publication-ready visualization. The swimmer plot visualization (Figure 1) effectively illustrated the censoring mechanism through patient-level timelines, distinguishing observed events (X markers) from censored observations (circles) across 20 representative patients with follow-up times ranging from 0.53 to 60.01 months. The integration of Kaplan-Meier curves with aligned number-at-risk tables (Figure 3) follows contemporary journal standards that enhance clinical interpretability by preventing misinterpretation of late-follow-up survival estimates based on inadequate sample sizes. The comprehensive validation of statistical assumptions through Schoenfeld residual analysis (Figure 2) demonstrates methodological rigor that strengthens confidence in reported effect estimates and supports their application to clinical decision-making.

Several limitations warrant acknowledgment in interpreting these findings. The synthetic dataset generated from exponential distributions with constant hazard rates may not capture the complex temporal patterns of real clinical outcomes, where hazards often vary substantially across follow-up periods. Equal randomization (200 patients per arm) and balanced baseline characteristics reflect

ideal trial conditions not universally achieved in practice, potentially underestimating real-world variability and selection bias. The relatively modest follow-up duration (median approximately 7-14 months) may not capture long-term treatment effects, late adverse events, or delayed immunological responses that could alter treatment rankings. Covariate adjustment limited to age and ECOG performance status does not account for other established prognostic factors such as tumor burden, histology, molecular markers, or comorbidities that could modify treatment effects or confound observed associations. The synthetic nature of the data precludes validation against actual clinical outcomes and external generalizability assessments.

Future research directions should prioritize prospective validation of these methodological approaches in real-world oncology trials with extended follow-up and comprehensive covariate assessment. Investigation of time-varying treatment effects through flexible parametric models or spline-based approaches could elucidate whether ImmunoX's advantage manifests uniformly across follow-up or concentrates in specific temporal windows. Biomarker-driven subgroup analyses would identify patient populations most likely to benefit from immunotherapy, enabling precision medicine approaches that maximize therapeutic efficacy while minimizing unnecessary treatment exposure. Health economic analyses comparing cost-effectiveness of ImmunoX versus chemotherapy would integrate survival gains with treatment costs and healthcare utilization patterns to inform resource allocation decisions. Comprehensive assessment of quality-of-life outcomes, treatment-related adverse events, and patient-reported outcomes would complement survival analyses to provide holistic evaluation of therapeutic value. The methodological framework demonstrated here-encompassing Kaplan-Meier estimation, multivariable Cox regression, proportional hazards validation, and publication-standard visualization-is readily generalizable to other time-to-event studies in oncology and diverse clinical domains, providing a template for rigorous survival analysis and transparent reporting that advances evidence-based medicine.

Acknowledgments

This article was generated using Digital Article, an open-source platform for reproducible data analysis and scientific writing. The platform combines computational analysis with AI-powered scientific writing to create publication-ready research articles. Digital Article is available at: github.com/lpalbou/digitalarticle

Article generated on February 01, 2026 at 10:30 UTC